THE JOURNAL OF BIOLOGICAL CHEMISTRY VOL. 285, NO. 25, pp. 19219–19226, June 18, 2010

Mapping the Ryanodine Receptor FK506-binding Protein Subunit Using Fluorescence Resonance Energy Transfer*[S]

Received for publication, September 18, 2009, and in revised form, March 11, 2010 Published, JBC Papers in Press, April 19, 2010, DOI 10.1074/jbc.M109.066944

Razvan L. Cornea[‡], Florentin R. Nitu[‡], Montserrat Samsó[§], David D. Thomas[‡], and Bradley R. Fruen[‡1]

From the [‡]Department of Biochemistry, Molecular Biology, and Biophysics, University of Minnesota, Minneapolis, Minnesota 55455 and the [§]Department of Anesthesiology, Perioperative and Pain Medicine, Brigham and Women's Hospital, Boston, Massachusetts 02115

The 12-kDa FK506-binding proteins (FKBP12 and FKBP12.6) are regulatory subunits of ryanodine receptor (RyR) Ca^{2+} release channels. To investigate the structural basis of FKBP interactions with the RyR1 and RyR2 isoforms, we used site-directed fluorescent labeling of FKBP12.6, ligand binding measurements, and fluorescence resonance energy transfer (FRET). Single-cysteine substitutions were introduced at five positions distributed over the surface of FKBP12.6. Fluorescent labeling at position 14, 32, 49, or 85 did not affect high affinity binding to the RyR1. By comparison, fluorescent labeling at position 41 reduced the affinity of FKBP12.6 binding by 10-fold. Each of the five fluorescent FKBPs retained the ability to inhibit [^{3}H]ryanodine binding to the RyR1, although the maximal extent of inhibition was reduced by half when the label was attached at position 32. The orientation of FKBP12.6 bound to the RyR1 and RyR2 was examined by measuring FRET from the different labeling positions on FKBP12.6 to an acceptor attached within the RyR calmodulin subunit. FRET was dependent on the position of fluorophore attachment on FKBP12.6; however, for any given position, the distance separating donors and acceptors bound to RyR1 *versus* RyR2 did not differ significantly. Our results show that FKBP12.6 binds to RyR1 and RyR2 in the same orientation and suggest new insights into the discrete structural domains responsible for channel binding and inhibition. FRET mapping of RyR-bound FKBP12.6 is consistent with the predictions of a previous cryoelectron microscopy study and strongly supports the proposed structural model.

The 2.3-MDa ryanodine receptor (RyR)[2]/Ca^{2+} release channel isoforms expressed in skeletal muscle (RyR1) and cardiac muscle (RyR2) function in complex with smaller regulatory proteins, which include FK506-binding proteins (FKBP12 and FKBP12.6) and calmodulin (CaM) (1, 2). The FKBPs tightly bind to RyR channels and may function to stabilize channels in a fully closed conformational state while minimizing the occurrence of subconductance states (3, 4).

Disruption of FKBP binding to RyRs has been proposed to underlie increased channel openings in response to β-adrenergic stimulation (5), oxidation/nitrosylation (6–8), or disease-causing channel mutations (9–11), and the FKBP binding interface is now under investigation as a therapeutic target for disordered Ca^{2+} regulation in cardiac and skeletal muscle. However, the fundamental cellular and molecular mechanisms that govern FKBP binding remain poorly defined, and the significance of reduced FKBP binding in RyR channelopathies is controversial (12–16). Because no atomic structure of an FKBP·RyR complex is currently available, uncertainty regarding the specific structural domains that comprise the binding interface remains a significant gap in understanding.

Molecular determinants of FKBP binding have been investigated previously through mutagenesis of FKBP12 and FKBP12.6 (17, 18). However, the key determinants thus far identified are broadly distributed throughout the FKBP three-dimensional structure and do not provide a clear indication of a major RyR binding interface. Cryoelectron microscopy (cryo-EM) and single-particle three-dimensional reconstruction of RyRs in the absence and presence of FKBP12/12.6 have demonstrated that the FKBPs bind within a pocket formed by the intersection of domains 3 and 9 of the RyR1 and RyR2 cytoplasmic assemblies (19, 20). More recently, Samsó *et al.* (21) advanced this approach to higher resolution and were able to dock the atomic structure of FKBP12 into the three-dimensional difference map of FKBP12 in a unique orientation. These results suggested a distinct mode of binding, in which the surface formed by the β-sheet and adjacent loops of FKBP12 forms a major binding interface with domain 9 of the RyR1 channel, and the hydrophobic drug-binding pocket of FKBP12 faces RyR1 domain 3.

Here, we extend an approach (22) based on site-directed labeling of channel regulatory proteins and fluorescence resonance energy transfer (FRET) to further investigate the structural basis of FKBP binding to RyR channels. We identify structural determinants of both high affinity binding and RyR inhibition. We define the orientation of FKBP12.6 when bound to both the RyR1 and the RyR2 channel isoforms. Our results provide the first FRET-based distance measurements within the cardiac RyR2 and demonstrate that distance relationships

* This work was supported, in whole or in part, by National Institutes of Health Grants R01HL076433 (to B. R. F.) and R01GM27906 (to D. D. T.). This work was also supported by a subcontract (to R. L. C.) from National Institutes of Health Grant R01HL092097 (to D. M. Bers, University of California, Davis, CA) and the BWH Biomedical Research Institute Fund to Sustain Research Excellence (to M. S.).

[S] The on-line version of this article (available at http://www.jbc.org) contains supplemental Figs. S1–S3.

[1] To whom correspondence should be addressed: 6-155 Jackson Hall, 321 Church St. SE, Minneapolis, MN 55455. Fax: 612-625-2163; E-mail: fruen001@umn.edu.

[2] The abbreviations used are: RyR, ryanodine receptor; FKBP, FK506-binding protein; FRET, fluorescence resonance energy transfer; CaM, calmodulin; SR, sarcoplasmic reticulum; cryo-EM, cryoelectron microscopy; MOPS, 3-(*N*-morpholino)propanesulfonic acid; PIPES, 1,4-piperazinediethanesulfonic acid; F-FKBP and F-CaM, fluorescence-labeled FKBP and CaM, respectively.

within the RyR1 and RyR2 isoforms are remarkably similar. Results are in excellent agreement with the mode of FKBP12-RyR1 binding predicted by previous cryo-EM studies (21).

EXPERIMENTAL PROCEDURES

Materials—Sarcoplasmic reticulum (SR) membrane vesicles were isolated from pig longissimus dorsi and pig ventricular tissue by differential ultracentrifugation of homogenized muscle (23). Cysteine-reactive fluorescent dyes were purchased from Invitrogen. [^{3}H]Ryanodine was from PerkinElmer Life Sciences. Image rendering of FKBP12, FKBP12.6, and RyR1 structural models was performed using the Chimera software package (24).

Expression, Purification, and Fluorescent Labeling of Single-cysteine Mutants of FKBP and CaM—Human FKBP12.6 cDNA was modified by site-directed mutagenesis (QuikChange kit, Stratagene (La Jolla, CA)) to introduce one of five different single-cysteine substitutions (T14C, N32C, D41C, R49C, or T85C) into a null cysteine background (C22A and C76I FKBP12.6). A single-cysteine FKBP12 was synthesized by introducing a T14C substitution into a null cysteine (C22A) FKBP12. FKBPs were expressed in *Escherichia coli* BL21(DE3)pLysS and purified on DEAE-Sephacel anion exchange and Sephacryl-200 HR columns, essentially as described (25, 26). FKBPs were labeled at their single cysteine using the maleimide derivatives of Alexa Fluor 488 or Alexa Fluor 555. Unreacted dye was separated from the fluorescence-labeled FKBPs (F-FKBPs) by phenyl-Sepharose chromatography, and the F-FKBPs were then dialyzed and concentrated using an Amicon device (YM3 filters, Millipore (Billerica, MA)) into 20 mM MOPS, 30 mM NaCl, pH 7.0. The degree of labeling of F-FKBPs was found to be ≥90%, based on the absorbance of the bound dye and the SDS-PAGE densitometry of the F-FKBP protein. Nearly stoichiometric labeling of F-FKBPs was confirmed by matrix-assisted laser desorption ionization time-of-flight mass spectrometry (supplemental Fig. S1*A*). Circular dichroism was performed to rule out major changes in FKBP12.6 secondary structure resulting from mutagenesis and fluorescent labeling (supplemental Fig. S1*B*). An F-CaM acceptor was synthesized by labeling a T34C CaM mutant at its single cysteine with Alexa Fluor 568, as described previously (27).

Binding Measurements—The binding of FKBPs to SR membranes (0.4 mg/ml) was measured following 90-min incubations in 37 °C buffer containing 150 mM KCl, 20 mM K-PIPES (pH 7.0), 5 mM GSH, 0.1 mg/ml bovine serum albumin, 1 mM EGTA, 1 mM $CaCl_2$ (30 μM free Ca^{2+}, calculated using Maxchelator), and 100 nM Alexa 555-labeled FKBP12. For determinations of nonspecific binding, 2 μM unlabeled FKBP12.6 was added to the binding buffer. Bound and free F-FKBP were separated by centrifugation at 100,000 × *g*. Pellets were dissolved in 5% SDS, 50 mM NaCl, 20 mM Na-PIPES (pH 7.0), and 1 mM EGTA. Bound Alexa 555-labeled FKBP12 was determined from the integrated fluorescence intensity from 563 to 591 nm, acquired using a Gemini EM microplate fluorometer (Molecular Devices, Sunnyvale, CA) with excitation at 542 nm and a 550-nm emission long pass filter (no contribution of Alexa 488-labeled FKBPs to the fluorescence signal).

For determinations of the FKBP dependence of [^{3}H]ryanodine binding, skeletal muscle SR membranes (0.1 mg/ml) were pretreated with 2 μM FK506 to remove endogenous FKBPs. Binding of [^{3}H]ryanodine (20 nM) was determined following 16-h incubations at 25 °C in KCl/PIPES buffer containing 0.2 mg/ml SR protein, as described previously (23). IC_{50} values are based on fits to the Hill equation.

FRET Measurements and Calculation of Donor-Acceptor Distances—FRET between RyR-bound F-FKBPs and F-CaM was measured as described previously (22) in KCl/PIPES buffers containing 30 μM Ca^{2+}. SR membranes (0.4 mg/ml) were preincubated with 50 nM Alexa 488-labeled FKBP12.6 (donor) for 90 min at 37 °C. Membranes were centrifuged at 100,000 × *g* to remove unbound donor, and the pellet was resuspended to a final concentration of 3 mg/ml. FRET was measured following 2.5-h incubations at 25 °C in the same buffer containing 0 – 800 nM Alexa 568-labeled CaM (acceptor).

Fluorescence emission spectra were acquired at 25 °C with excitation at 490 nm, and a 495-nm emission long pass filter. Donor-only samples and acceptor-only samples displayed distinct emission maxima at 518 and 600 nm, respectively (supplemental Fig. S2). FRET efficiency was calculated from the decrease in donor steady-state fluorescence (F_D) due to the presence of acceptor (F_{DA}) according to Equation 1,

$$\mathrm{FRET} = \left(1 - \frac{F_{DA}}{F_D}\right) \qquad \text{(Eq. 1)}$$

To verify that FRET was strictly dependent on donor binding, control experiments measured FRET in samples that contained either FK506 or unlabeled FKBP12.6 to block F-FKPB binding to RyRs (supplemental Fig. S2). Alternatively, excess unlabeled CaM was added to block binding of the F-CaM acceptor and abolish FRET.

Donor-acceptor distances, *R*, were calculated from Equation 2,

$$R = R_0(\mathrm{FRET}^{-1} - 1)^{1/6} \qquad \text{(Eq. 2)}$$

where the Förster distance, R_0, is defined as the distance at which FRET = 0.5 (62 Å for the Alexa 488-Alexa 568 donor-acceptor pair) (28).

To assign a unique orientation to the RyR-bound FKBP relative to the CaM subunit, we assumed that observed FRET efficiencies are primarily a function of the proximity of each F-FKBP donor to its nearest neighbor F-CaM acceptor bound to the same lateral face of the RyR and that any FRET to F-CaMs bound to different faces of the same channel, to neighboring channels, or to non-RyR targets had comparatively little impact on the aggregate FRET signal. This assumption is well supported by the disposition of FKBP and CaM subunits in cryo-EM structures (19), by our own previous analysis (22), and by the donor-acceptor distances derived in this study (Table 1). A schematic is included to illustrate the predicted distance relationships among multiple donors and acceptors bound within an ordered array of RyR channels, in the context of the limited range of distances over which FRET may occur (supplemental Fig. S3).

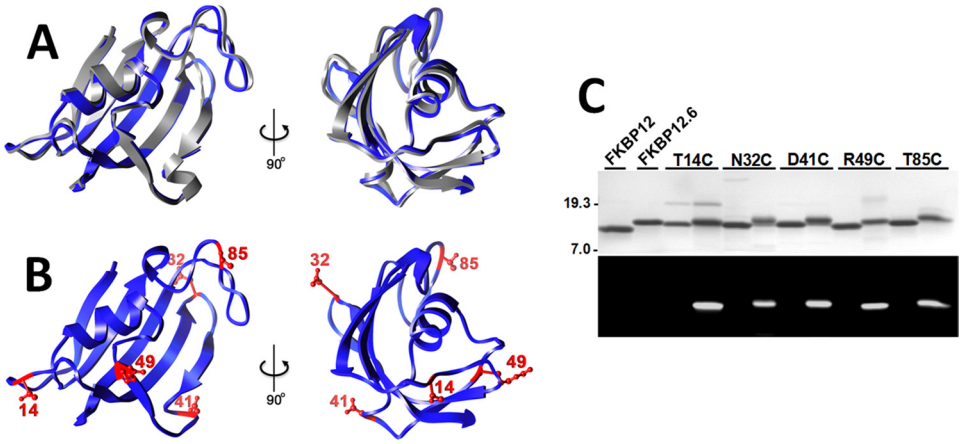

FIGURE 1. **Structure and site-directed fluorescent labeling of FKBP12.6.** *A*, the structure of FKBP12.6 (*blue*; Protein Data Bank entry 1C9H) is superimposed with FKBP12 (*gray*; Protein Data Bank entry 1D6O) for comparison. *B*, five FKBP12.6 residues targeted for cysteine mutagenesis and fluorescent labeling are shown in *red*. *C*, SDS-PAGE of the five single-cysteine FKBP12.6 mutants and their corresponding fluorescent conjugates (*above*, Coomassie; *below*, fluorescence). *Lanes 1* and *2* contain wild-type FKBP12 and FKBP12.6, respectively, as standards.

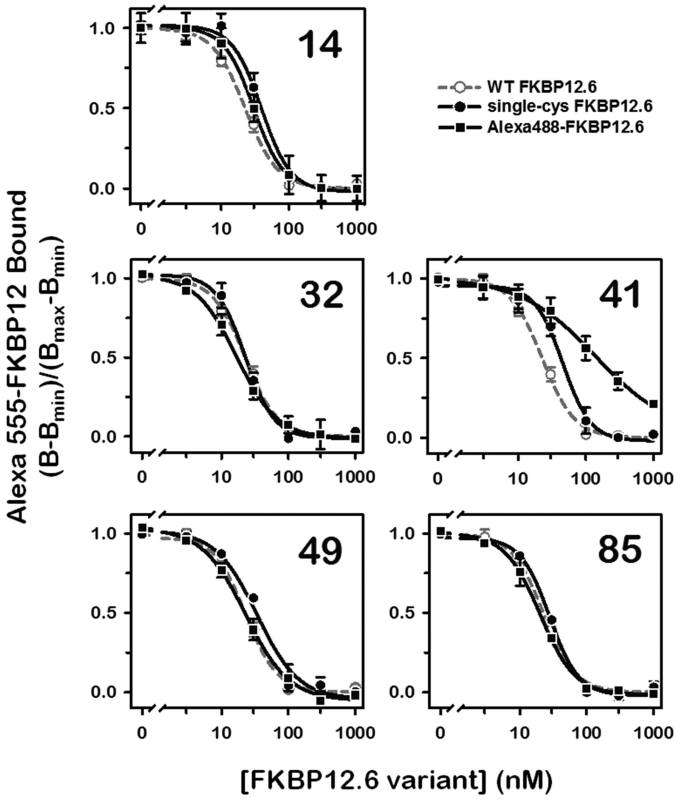

FIGURE 2. **Competitive inhibition of FKBP12 binding to the skeletal muscle RyR1 by five single-cysteine mutants of FKBP12.6 and their fluorescent conjugates.** Skeletal muscle SR membranes were incubated in medium containing Alexa 555-labeled FKBP12 (100 nM) and a 0–1000 nM concentration of an FKBP12.6 modified at either position 14, 32, 41, 49, or 85, as denoted in the *upper right* of each *graph*. Normalized membrane-bound fluorescence data are means ± S.E. (*error bars*) from 3–5 experiments (excitation 542 nm, emission 563–591 nm).

Statistics—Sample means are from two or more independent experiments. Experiments were repeated using at least two independent SR membrane preparations, isolated from different animals. Means were compared using Student's *t* test and considered significantly different at $p < 0.05$.

RESULTS

FKBP12 and FKBP12.6 share 85% amino acid sequence homology and nearly identical backbone structures (Fig. 1*A*) (29). The FKBP12 isoform is more widely and abundantly expressed and copurifies with the RyR1 channel from mammalian skeletal muscle, where FKBP12.6 is absent. However, *in vitro* FKBP12.6 binds with higher affinity and selectivity to both the RyR1 and RyR2 channels (17) and thus provides an ideal means of targeting fluorescent probes to each of the two channel isoforms (22).

To determine the orientation at which FKBPs bind to RyR1 and RyR2 channels and to identify key FKBP domains at the binding interface, we synthesized a series of fluorescence-labeled FKBP12.6 mutants. Single-cysteine substitutions were introduced at five positions distributed over the surface of FKBP12.6 (Fig. 1*B*). We selected for modification only solvent-exposed side chains outside the FKBP hydrophobic core, to minimize potential effects of mutagenesis and fluorescent labeling on global tertiary structure. Each of the five single-cysteine FKBPs was individually labeled with green fluorescent Alexa 488. SDS-PAGE analysis demonstrated single fluorescent bands for each of the five F-FKBPs, with apparent molecular masses slightly greater than the corresponding unlabeled single-cysteine FKBPs (Fig. 1*C*).

Competition Studies of F-FKBP Binding to SR Membranes—To identify FKBP12.6 mutants and fluorescent conjugates that retained high affinity binding to RyR1 channels, we examined the competitive inhibition of FKBP12 binding to skeletal muscle SR membranes (Fig. 2). FKBP12 was labeled with red fluorescent Alexa 555. In the absence of FKBP12.6, SR membranes bound 55.7 ± 5.8 pmol of Alexa 555-FKBP12/mg of protein, consistent with a binding stoichiometry of four FKBP12 per RyR1 tetramer (30). The addition of wild-type, unlabeled FKBP12.6 fully inhibited FKBP12 binding (Fig. 2, *dashed gray lines*; IC_{50} = 22.6 ± 2.2 nM), demonstrating that the two FKBP isoforms competed at a common binding site on the RyR1.

The introduction of a single cysteine at position 14, 32, 49, or 85 did not significantly alter the concentration dependence of FKBP12.6 inhibition (Fig. 2, *blue lines*). Furthermore, high affinity binding was retained following the covalent attachment of Alexa 488 at each of these four positions (*green lines*), suggesting that positions 14, 32, 49, and 85 are removed from the major RyR1 binding interface.

By comparison, the introduction of a cysteine at position 41 resulted in a significant rightward shift in the FKBP12.6 dependence of inhibition (IC_{50} = 45.4 ± 5.4 nM, p = 0.01). Attachment of fluorophore at this position evoked a further rightward shift in FKBP12.6 inhibition (IC_{50} > 100 nM). Circular dichroism indicated that FKBP12.6 secondary structure was unaffected by fluorescent labeling at position 41

(supplemental Fig. S1*B*). Thus, the marked decrease in RyR1 binding affinity that resulted from labeling at position 41 may be explained by steric hindrance in the vicinity of the major binding interface.

RyR1 Inhibition by F-FKBPs—To identify fluorescence-labeled FKBPs that retained the ability to inhibit the RyR1 channels, we characterized the inhibition of [^{3}H]ryanodine binding to skeletal muscle SR membranes by the different F-FKBPs. Initial experiments characterized the effects of wild-type FKBP12 and FKBP12.6 on the Ca^{2+} dependence of [^{3}H]ryanodine binding to SR membranes that had been pretreated with FK506 to remove native FKBP12. The addition of unlabeled FKBP12 decreased the Ca^{2+} activation of [^{3}H]ryanodine binding to the FKBP-depleted membranes by approximately half (Fig. 3*A*). Unlabeled FKBP12.6 evoked a similar decrease in [^{3}H]ryanodine binding. Fig. 3*B* compares the inhibition of [^{3}H]ryanodine binding by the five single-cysteine FKBP mutants and their fluorescent conjugates. All of the FKBP variants significantly inhibited [^{3}H]ryanodine binding. However, fluorescent labeling at position 32 significantly reduced the extent of RyR1 inhibition.

Subsequent experiments further examined the concentration-dependent inhibition of [^{3}H]ryanodine binding by the F-FKBPs labeled at positions 32 and 41. Results (Fig. 3*C*) verified that fluorescent labeling at position 32 reduced by half the inhibitory effect observed at high F-FKBP concentrations. Thus, although competition studies (Fig. 2) indicated that this F-FKBP retained high affinity binding to the RyR1, results shown in Fig. 3, *B* and *C*, indicate that the F-FKBP labeled at position 32 was impaired in its ability to inhibit the RyR1 when bound to the channel.

Fluorescent labeling at position 41, on the other hand, did not alter the maximal extent of RyR1 inhibition (Fig. 3*C*). Rather, labeling at this position only increased the FKBP concentration required for RyR1 inhibition (IC_{50} = 83.1 ± 19 nM *versus* 17.1 ± 2.9 nM for D41C F-FKBP and unlabeled wild-type FKBP12.6, respectively; p = 0.01). Results from [^{3}H]ryanodine binding and competition studies are therefore consistent in indicating that the F-FKBP labeled at position 41 binds to the RyR1 with a markedly reduced affinity yet retains full efficacy in inhibiting the RyR1 at sufficiently high concentrations. Taken together, our [^{3}H]ryanodine binding (Fig. 3) and competition studies (Fig. 2) indicate that site-directed modifications of FKBP12.6 may independently alter either functional activity (position 32) or high affinity binding (position 41).

Orientation of F-FKBPs Bound to RyR1 and RyR2 Revealed Using FRET—We used FRET to examine distance relationships between Alexa 488 (donor) attached at the different positions on FKBP12.6 and Alexa 568 (acceptor) attached to the RyR CaM subunit. Skeletal muscle SR membranes were preincubated with the different F-FKBPs and washed to remove unbound F-FKBP donor. Representative emission spectra for each of the five F-FKBPs bound to the RyR1 channel isoform are shown in Fig. 4*A*. Upon excitation at 490 nm, donor-only samples (*green lines*) displayed a single fluorescence peak at 518 nm. A second fluorescence peak at 600 nm was apparent in samples that contained both donor and acceptor (800 nM, *red lines*).

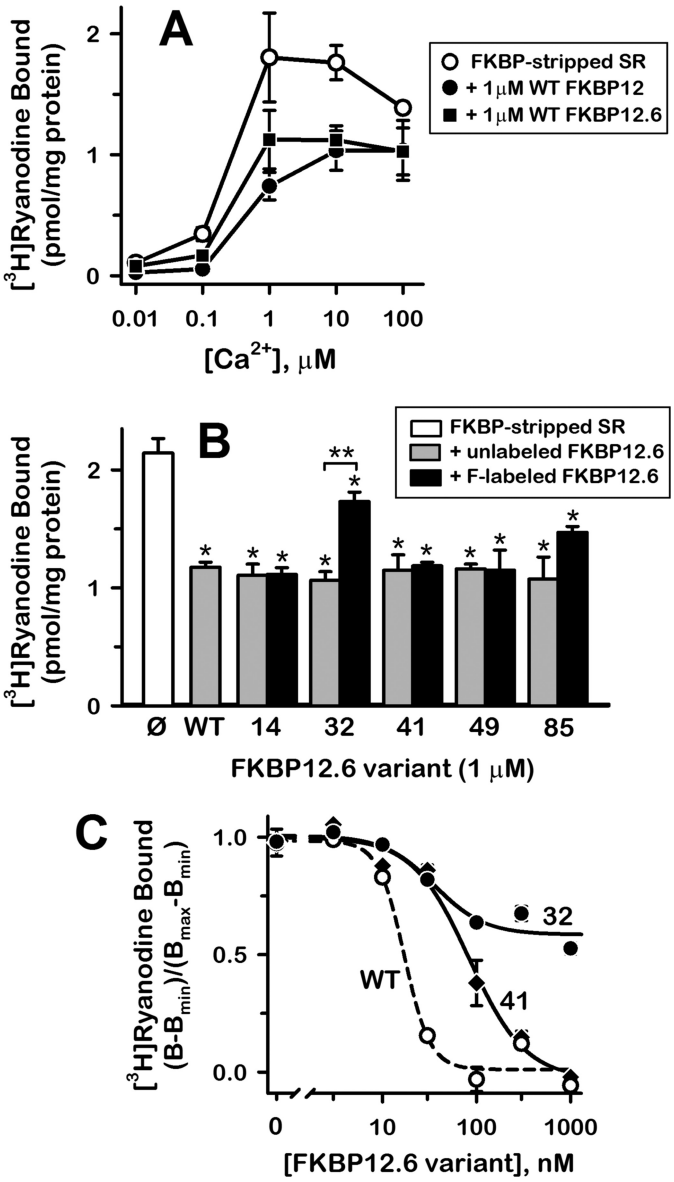

FIGURE 3. **Effects of cysteine mutagenesis and fluorescent labeling on FKBP inhibition of [^{3}H]ryanodine binding to RyR1 channels.** *A*, [^{3}H]ryanodine binding to skeletal muscle SR membranes pretreated with FK506 (2 μM) was determined in the absence or presence of either wild type FKBP12 (*WT-FKBP12*) or FKBP12.6 (*WT-FKBP12.6*) (unlabeled proteins). *B*, inhibition of ryanodine binding by single-cysteine FKBP12.6 mutants and their fluorescent conjugates (1 μM) was determined in 10 μM Ca^{2+}. Samples contained either no FKBP (Ø), unlabeled wild type FKBP12.6 (*WT*), or an FKBP variant modified at position 14, 32, 41, 49, or 85, as indicated. *, denote significant difference from samples containing no FKBP; **, significant differences from samples containing wild-type FKBP12.6 ($p < 0.05$). *C*, concentration dependence of RyR1 inhibition by unlabeled wild-type FKBP12.6 (*open circles*), Alexa 488-labeled N32C FKBP12.6 (*closed circles*), and Alexa 488-labeled D41C FKBP12.6 (*diamonds*). Data are means ± S.E. (*error bars*) from two experiments (*A*) or from three or four experiments (*B* and *C*).

FRET was evident as a decrease in the fluorescence of the RyR1-bound donor in the presence of the acceptor. The magnitude of the FRET signal differed depending on the position of donor attachment on FKBP12.6. FRET was greatest when the donor was attached at position 49 and least when the donor was attached at position 32 or 41 (Fig. 4*A*). In each case, FRET was abolished when the specific binding of acceptors to RyR1 channels was blocked by the addition of excess unlabeled CaM (*gray lines*).

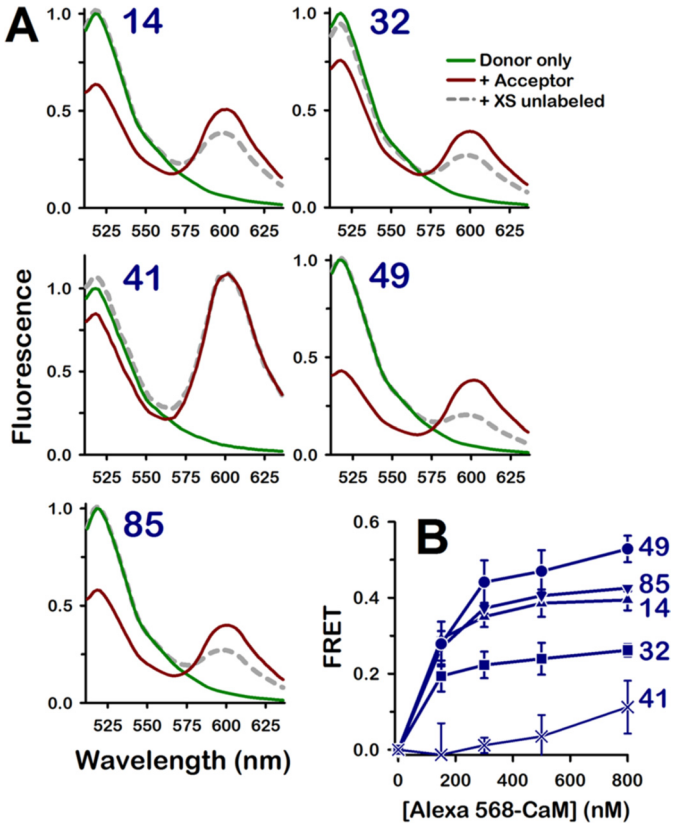

FIGURE 4. **FRET between F-FKBPs (donor) and F-CaM (acceptor) bound to the skeletal muscle RyR1 channel.** *A*, representative spectra from experiments in which the Alexa 488 donor was attached at either position 14, 32, 41, 49, or 85 of FKBP12.6, as indicated in the individual *graphs*. Samples contained skeletal muscle SR membranes (3 mg/ml) and donor only (*green*), donor plus acceptor (800 nM; *red*), or donor plus acceptor plus excess unlabeled CaM (16 μM; *gray*). All spectra are normalized to donor-only fluorescence at 518 nm. Consequently, in the case of the F-FKBP labeled at position 41, a reduced donor signal (attributable to decreased F-FKBP binding) is reflected as a relative increase in F-CaM acceptor fluorescence at 600 nm. *B*, FRET, calculated as the fractional decrease in donor fluorescence, is plotted as a function of acceptor concentration. *Numbers* at the *right* indicate the position of donor attachment on FKBP12.6. Data are means ± S.E. (*error bars*) from four experiments.

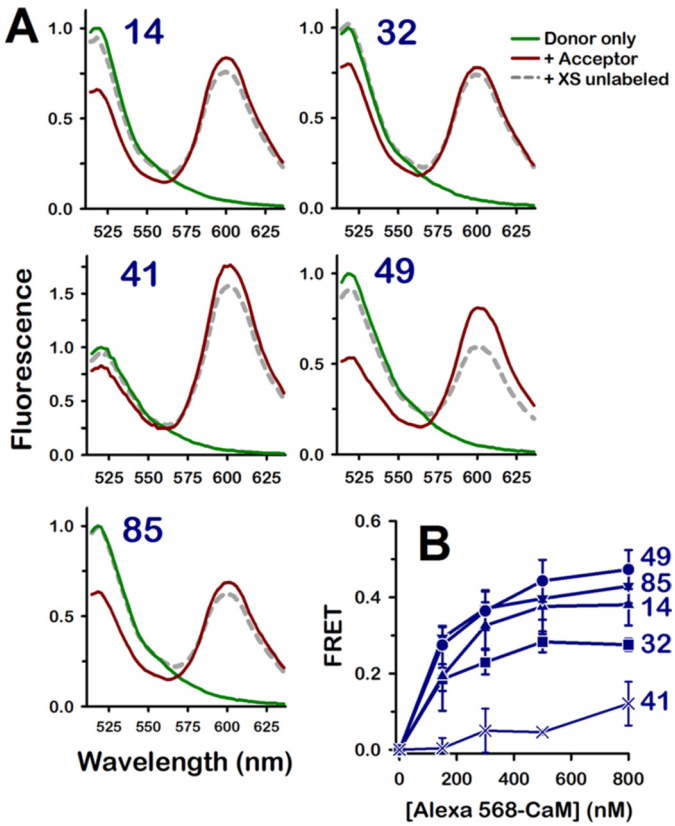

FIGURE 5. **FRET between fluorescence-labeled FKBP12.6 and CaM bound to the cardiac RyR2 channel.** *A*, representative spectra from experiments in which the Alexa 488 donor was attached at position 14, 32, 41, 49, or 85 of FKBP12.6, as indicated. Samples contained 3 mg/ml cardiac SR and donor only (*green*), donor plus 800 nM acceptor (*red*), or donor plus acceptor plus 16 μM unlabeled CaM (*gray*). *B*, FRET from the different positions on FKBP12.6 is plotted as a function of acceptor concentration (means ± S.E. (*error bars*) from 3–6 experiments).

RyR1 FRET experiments are summarized in Fig. 4*B*, in which FRET from each of the five positions on FKBP12.6 is plotted as a function of Alexa 568-CaM acceptor concentration. Note that FRET from positions 14, 32, 49, and 85 increased sharply with the addition of acceptor and reached saturation at concentrations of ≥300 nM. We therefore conclude that FRET from these positions on FKBP12.6 provided a direct indication of acceptor binding at saturable, high affinity CaM sites in close proximity to the RyR1 FKBP site. We attribute differences in maximal FRET observed at saturating acceptor concentrations to differences in the proximity of the donor when attached at position 14, 32, 49, or 85.

Weak energy transfer was observed in measurements using the F-FKBP labeled at position 41 (Fig. 4*B*, FRET ≤0.11). This observation may be taken to indicate that the donor attached at position 41 is oriented furthest from the acceptor when bound within the macromolecular RyR1. Alternatively, the absence of a robust FRET signal in these measurements may reflect the partial dissociation of this F-FKBP from the RyR1 during 2.5-h incubations with the FRET acceptor. This latter possibility is supported by the reduced RyR1 binding affinity of the F-FKBP labeled at position 41 that was demonstrated in our binding studies (Figs. 2 and 3). Reduced binding of this F-FKBP is also evident in the spectra in Fig. 4*A*, in which the amplitude of the donor fluorescence peak for this F-FKBP is clearly decreased relative to that of the acceptor. We therefore conclude that the absence of a robust FRET signal when the donor was attached at position 41 is in part attributable to the reduced affinity of this F-FKBP for the RyR1.

We also examined FRET between FKBPs and CaM bound to the cardiac RyR2 channel, to determine how donor-acceptor proximities compare across the different RyR isoforms. Cardiac SR membranes were preincubated with the Alexa 488-labeled FKBPs and washed to remove unbound F-FKBP donor. Binding of each of the five F-FKBPs was evidenced by fluorescence at 518 nm (Fig. 5*A*, *green lines*). A decrease in F-FKBP donor fluorescence upon the addition of the F-CaM acceptor (*red lines*) indicated FRET between RyR2-bound donors and acceptors.

Summarized data (Fig. 5*B*) demonstrate that FRET efficiencies obtained using cardiac SR membranes were remarkably similar to those when using skeletal muscle SR (Fig. 4*B*). For example, when the donor was attached at position 49, the FRET signal at 800 nM acceptor was 0.47 ± 0.05 using cardiac SR membranes and 0.53 ± 0.04 using skeletal muscle SR mem-

TABLE 1

Distance relationships between the Alexa 488 donor attached at different positions on FKBP12.6 and the Alexa 568 acceptor attached to CaM

Distances are derived from Equation 1 and FRET observed in the presence of 800 nM Alexa 568-CaM (Figs. 4*B* and 5*B*). ND, value not determined. Pos., position.

	Distance (Å)				
	Pos. 14	Pos. 32	Pos. 41	Pos. 49	Pos. 85
RyR1	67 ± 3	77 ± 3	ND	61 ± 3	65 ± 2
RyR2	67 ± 5	74 ± 3	ND	63 ± 4	65 ± 2

branes ($p = 0.4$). Furthermore, the relative efficiencies of energy transfer from the five positions on FKBP12.6 were the same whether FRET probes were bound to cardiac or skeletal muscle SR membranes (position 49 > 85 ≥ 14 > 32 > 41). Thus, our FRET results indicate that in binding the RyR1 and RyR2 isoforms, FKBP12.6 adopts the same orientation, in which position 49 is located nearest to the adjacent CaM subunit.

Analysis of Donor-Acceptor Distances—FRET provides a sensitive measure of donor-acceptor distances in the range of 0.5–1.5 × R_0. Given a Förster radius of 62 Å for the donor-acceptor pair in our FRET experiments (28), we calculated the distances separating donors attached at different positions on FKBP12.6 from the acceptor attached within the N-lobe of CaM (Table 1). This analysis excluded results obtained using the F-FKBP labeled at position 41 because we considered that the uncoupling of donors and acceptors due to reduced F-FKBP binding contributed to the weak FRET from position 41. Distances between donors and acceptors bound to the RyR1 isoform ranged from 61 Å when the donor was attached at position 49 of FKBP12.6 to 77 Å when the donor was attached at position 32. Distances between donors and acceptors bound to the cardiac RyR2 isoform were very similar and did not significantly differ from the corresponding RyR1 distances for any given position on FKBP12.6.

DISCUSSION

Uncertainty regarding the structural basis of FKBP binding to RyR channels has contributed to the controversy that surrounds the molecular mechanisms controlling these interactions in cardiac and skeletal muscle. By attaching a donor fluorophore at discrete positions on FKBP12.6 and measuring FRET to the RyR CaM subunit, we have determined the orientation of FKBP12.6 binding within the cytoplasmic assembly of the RyR1 and RyR2 channel isoforms. Previously, we used this approach to define the orientation of CaM binding within the RyR1 (22).

Orientation of F-FKBPs Bound to RyR1—Our FRET results are in excellent agreement with the mode of FKBP12 binding to RyR1 channels predicted by the previous cryo-EM studies of Samsó *et al.* (21). For example, note that in the cryo-EM model (Fig. 6), Met^{49} of FKBP12 faces away from the major binding interface and is thereby situated nearest to the putative site of CaM binding across RyR1 domain 3 (19). Accordingly, we found that energy transfer to CaM was strongest when the donor was attached at position 49 on FKBP12.6 (Fig. 4*B*). By comparison, Glu^{32} lies opposite to Met^{49} on the FKBP12 surface and points away from the CaM binding site in the cryo-EM model. Accordingly, we observed weaker FRET when the donor fluorophore was attached at position 32 (Fig. 4*B*).

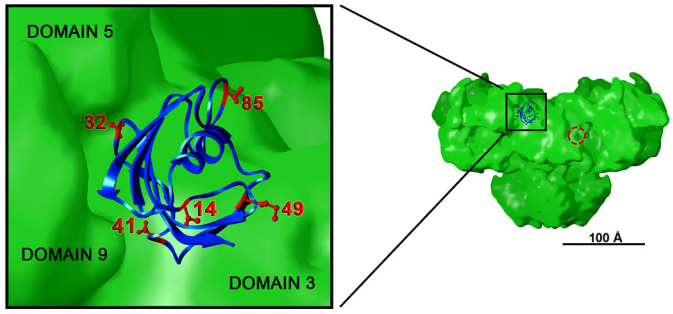

FIGURE 6. **Cryo-EM model of FKBP12 binding within the three-dimensional architecture of the RyR1 channel showing the predicted orientation of FKBP relative to the F-CaM acceptor.** The RyR1 (*green*) is shown in *side view*. FKBP12 (*blue*) is shown with the five positions targeted for donor fluorophore attachment in this study *highlighted* in *red*. The *red circle* at the *right* indicates the predicted position of the fluorescent acceptor attached within the N-lobe of CaM (19, 22). This figure was adapted from Ref. 21.

Although positions 14 and 85 are widely separated in the FKBP12/12.6 atomic structures (Fig. 1*A*), we found that FRET from these two positions was similar and intermediate to that from positions 49 and 32. This result is also consistent with the model in Fig. 6, in which residues Thr^{14} and Thr^{85} of FKBP12 are situated roughly equidistant from the F-CaM acceptor. All distance determinations (Table 1) were well within expected limits based on the dimensions of the RyR cytoplasmic assembly (280 × 280 × 120 Å), the separation of nearest neighbor FKBP and CaM subunits in cryo-EM models (19, 31), the sizes of the donor and acceptor fluorophores and their flexible linkers (28), and our own previous determinations (22) (see also supplemental Fig. S3). Thus, our FRET results indicate that FKBP12.6 binds to the RyR1 in the orientation predicted for FKBP12 binding using cryo-EM. Excellent agreement between these very different structural approaches and different channel preparations strongly supports the validity of this model of FKBP·RyR binding.

Determinants of RyR1 Binding and Inhibition by F-FKBPs—Additional insights into the mode of FKBP binding were provided by competition studies identifying the effects of single cysteine substitutions and their fluorescent conjugates on high affinity binding to the RyR1. We found that binding was unaffected by modifications at four of five positions on FKBP12.6 (Fig. 2), indicating that these positions are removed from the major binding interface. In contrast, labeling at position 41 resulted in an ~10-fold decrease in binding affinity, indicating that key determinants of high affinity binding are localized to this region. In support of this conclusion, the cryo-EM model shows Asp^{41} pointing toward the interface of FKBP12 with RyR1 domain 9.

Remarkably, modifications at position 41 did not affect the efficacy of FKBP12.6 as an inhibitor of [^{3}H]ryanodine binding (Fig. 3*C*). This suggests that, although determinants of high affinity binding are localized near Asp^{41} of FKBP12.6, contacts critical for channel regulation involve distinct structural domains. Previously, Huang *et al.* (32) reported that removal of negatively charged aspartate residues at positions 37 and 41 enhanced FKBP12.6 binding to a mutant RyR2 that mimics a

constitutively phosphorylated channel (RyR2 S2808D). Although the current results and those of Huang *et al.* (32) are not directly comparable, both studies suggest that contacts in the vicinity of Asp^{41} comprise a key component of the binding interface. This conserved region of FKBP12/12.6 contains a phosphorylation motif (^{34}KKFDS SRD^{41}), and protein kinase C phosphorylation of FKBP12 has been demonstrated *in vitro* (33). However, no study to date has demonstrated phosphorylation of FKBP12/12.6 *in vivo*.

In the cryo-EM model, Asp^{32} of FKBP12 points toward the intersection of RyR1 domains 5 and 9 and lies very near the edge of the binding interface. Therefore, we were surprised that the F-FKBP labeled at position 32 retained an affinity for the RyR1 comparable with that of unlabeled wild-type FKBP12.6 (Fig. 2). Position 32 marks a region of FKBP12/12.6 sequence divergence, in which residues Glu^{31} and Asp^{32} in FKBP12 are replaced by their corresponding amines in FKBP12.6. The resultant charge difference has previously been suggested to account for isoform differences in FKBP12/12.6 binding and regulation of RyR channels (17). The above model places these residues adjacent to the RyR1 "clamp" region, which is thought to be a major site for the allosteric modulation of channel activity (2). In this regard, we found that fluorescent labeling at position 32 markedly reduced the efficacy of FKBP12.6 in inhibiting [^{3}H]ryanodine binding to the RyR1 (Fig. 3). We conclude that structural determinants in the vicinity of position 32 may contribute to the productive interactions of FKBP with a regulatory site in the RyR clamp region yet lie outside the major interface responsible for high affinity binding to RyRs. Additional modifications of this region might therefore yield novel, functionally inert antagonists of the FKBP regulatory site.

F-FKBPs Bind to RyR1 and RyR2 in the Same Orientation—Direct comparisons of F-FKBP interactions with RyR1 and RyR2 channels were made possible by synthesizing F-FKBPs derived from the FKBP12.6 isoform, which binds to both RyR1 and RyR2 with high affinity. We found that FRET in samples containing the cardiac RyR2 (Fig. 5*B*) was essentially equivalent to that observed in the presence of the skeletal muscle RyR1 (Fig. 4*B*). This result is noteworthy not only because of the differences in the channel isoforms to which donors and acceptors bound but also because of the different background of non-RyR proteins present in cardiac and skeletal SR membranes that may potentially interact with our fluorescent proteins. The F-CaM acceptor, in particular, is expected to bind to multiple membrane targets (22), and the identity and concentrations of these targets will differ between cardiac and skeletal SR. The very similar FRET that we observed using cardiac and skeletal muscle membranes therefore supports our previous conclusion (22) that FRET in our assays is a function of the proximity of donors and acceptors bound to RyR channels and that acceptor binding at non-RyR CaM sights does not contribute significantly to the FRET signal. Our results further showed that the rank order of FRET from the different positions on FKBP was the same for RyR1 and RyR2. This demonstrates for the first time that FKBP12.6 binds to the different channel isoforms in the same orientation.

Donor-acceptor distances derived from FRET measurements revealed no significant differences between RyR1 and RyR2 for any given position of donor attachment on FKBP12.6 (Table 1). This result is consistent with the essentially identical three-dimensional architectures of the two channel isoforms at 20–30 Å resolutions (2, 34) and with the similar dispositions of their FKBP and CaM subunits. Although the comprehensive ligand-binding studies used to characterize the different F-FKBP interactions with the RyR1 isoform were not extended to the RyR2, these FRET results are strong evidence that the RyR2 isoform shares a common mode of FKBP binding with the RyR1 channel. In particular, the reduced donor fluorescence and low outlying FRET that was observed when the donor was attached at position 41 suggest that this F-FKBP also bound weakly to the RyR2 (Fig. 5), as was demonstrated directly for the RyR1 isoform in competitive binding studies (Fig. 2).

Previous studies have documented important differences in the affinity and functional activity of FKBP12 and FKBP12.6 (17, 35, 36). These differences are probably a function of both the FKBP isoform and the RyR isoform, and understanding these differences remains an important goal. The present findings indicate that these differences are not linked to major differences in the orientation or mode of FKBP binding to RyR1 and RyR2. In a recent study, Guo *et al.* (37) examined the subcellular distribution and functional activity of F-FKBPs in permeabilized cardiac myocytes. Their results show that fluorescent conjugates of both FKBP12 and FKBP12.6 localized to the Z-line, consistent with specific binding to RyR2 channels. However, a significant inhibition of Ca^{2+} spark frequency was observed only in the presence of the FKBP12.6 isoform.

In conclusion, we describe the first use of site-directed labeling and FRET to map FKBP binding on RyR channels. Our results reveal that FKBP12.6 binds to RyR1 and RyR2 channels in the same orientation and yield new insights into the structural determinants of FKBP binding and regulation. Newly characterized F-FKBPs offer powerful tools for monitoring FKBP binding and regulation *in situ* and for targeting spectroscopic biosensors to the RyR N-terminal cytoplasmic domain. With recent progress in obtaining crystal structures of the RyR N-terminal domains (38, 39), a clearer picture of the FKBP binding interface is emerging.

Acknowledgments—We are grateful to Katherine Kohler, Mallory Turner, and Sinziana Cornea for excellent technical assistance, to Don Bers and Tao Guo for helpful discussions, and to the departmental biophysical spectroscopy facility for core instrumentation.

REFERENCES

1. Bers, D. M. (2004) *J. Mol. Cell. Cardiol.* **37,** 417–429
2. Hamilton, S. L., and Serysheva, I. I. (2009) *J. Biol. Chem.* **284,** 4047–4051
3. Brillantes, A. B., Ondrias, K., Scott, A., Kobrinsky, E., Ondriasová, E., Moschella, M. C., Jayaraman, T., Landers, M., Ehrlich, B. E., and Marks, A. R. (1994) *Cell* **77,** 513–523
4. Mayrleitner, M., Timerman, A. P., Wiederrecht, G., and Fleischer, S. (1994) *Cell Calcium* **15,** 99–108
5. Marx, S. O., Reiken, S., Hisamatsu, Y., Jayaraman, T., Burkhoff, D., Rosemblit, N., and Marks, A. R. (2000) *Cell* **101,** 365–376
6. Aracena, P., Tang, W., Hamilton, S. L., and Hidalgo, C. (2005) *Antioxid. Redox Signal.* **7,** 870–881
7. Zissimopoulos, S., Docrat, N., and Lai, F. A. (2007) *J. Biol. Chem.* **282,** 6976–6983

8. Bellinger, A. M., Reiken, S., Carlson, C., Mongillo, M., Liu, X., Rothman, L., Matecki, S., Lacampagne, A., and Marks, A. R. (2009) *Nat. Med* **15,** 325–330
9. Lehnart, S. E., Wehrens, X. H., Laitinen, P. J., Reiken, S. R., Deng, S. X., Cheng, Z., Landry, D. W., Kontula, K., Swan, H., and Marks, A. R. (2004) *Circulation* **109,** 3208–3214
10. Wehrens, X. H., Lehnart, S. E., Huang, F., Vest, J. A., Reiken, S. R., Mohler, P. J., Sun, J., Guatimosim, S., Song, L. S., Rosemblit, N., D'Armiento, J. M., Napolitano, C., Memmi, M., Priori, S. G., Lederer, W. J., and Marks, A. R. (2003) *Cell* **113,** 829–840
11. Serysheva, I. I., Ludtke, S. J., Baker, M. L., Cong, Y., Topf, M., Eramian, D., Sali, A., Hamilton, S. L., and Chiu, W. (2008) *Proc. Natl. Acad. Sci. U.S.A.* **105,** 9610–9615
12. Zissimopoulos, S., Thomas, N. L., Jamaluddin, W. W., and Lai, F. A. (2009) *Biochem. J.* **419,** 273–278
13. Xiao, J., Tian, X., Jones, P. P., Bolstad, J., Kong, H., Wang, R., Zhang, L., Duff, H. J., Gillis, A. M., Fleischer, S., Kotlikoff, M., Copello, J. A., and Chen, S. R. (2007) *J. Biol. Chem.* **282,** 34828–34838
14. Liu, N., Colombi, B., Memmi, M., Zissimopoulos, S., Rizzi, N., Negri, S., Imbriani, M., Napolitano, C., Lai, F. A., and Priori, S. G. (2006) *Circ. Res.* **99,** 292–298
15. Meng, X., Xiao, B., Cai, S., Huang, X., Li, F., Bolstad, J., Trujillo, R., Airey, J., Chen, S. R., Wagenknecht, T., and Liu, Z. (2007) *J. Biol. Chem.* **282,** 25929–25939
16. Bers, D. M. (2006) *Biochem. J.* **396,** e1–e3
17. Xin, H. B., Rogers, K., Qi, Y., Kanematsu, T., and Fleischer, S. (1999) *J. Biol. Chem.* **274,** 15315–15319
18. Lee, E. H., Rho, S. H., Kwon, S. J., Eom, S. H., Allen, P. D., and Kim, D. H. (2004) *J. Biol. Chem.* **279,** 26481–26488
19. Wagenknecht, T., Radermacher, M., Grassucci, R., Berkowitz, J., Xin, H., and Fleischer, S. (1997) *J. Biol. Chem.* **272,** 32463–32471
20. Sharma, M. R., Jeyakumar, L. H., Fleischer, S., and Wagenknecht, T. (2006) *Biophys. J.* **90,** 164–172
21. Samsó, M., Shen, X., and Allen, P. D. (2006) *J. Mol. Biol.* **356,** 917–927
22. Cornea, R. L., Nitu, F., Gruber, S., Kohler, K., Satzer, M., Thomas, D. D., and Fruen, B. R. (2009) *Proc. Natl. Acad. Sci. U.S.A.* **106,** 6128–6133
23. Fruen, B. R., Black, D. J., Bloomquist, R. A., Bardy, J. M., Johnson, J. D., Louis, C. F., and Balog, E. M. (2003) *Biochemistry* **42,** 2740–2747
24. Pettersen, E. F., Goddard, T. D., Huang, C. C., Couch, G. S., Greenblatt, D. M., Meng, E. C., and Ferrin, T. E. (2004) *J. Comput. Chem.* **25,** 1605–1612
25. Park, S. T., Aldape, R. A., Futer, O., DeCenzo, M. T., and Livingston, D. J. (1992) *J. Biol. Chem.* **267,** 3316–3324
26. Holzman, T. F., Egan, D. A., Edalji, R., Simmer, R. L., Helfrich, R., Taylor, A., and Burres, N. S. (1991) *J. Biol. Chem.* **266,** 2474–2479
27. Fruen, B. R., Balog, E. M., Schafer, J., Nitu, F. R., Thomas, D. D., and Cornea, R. L. (2005) *Biochemistry* **44,** 278–284
28. Haugland, R., Spence, M., Johnson, I., and Basey, A. (2005) *The Handbook: A Guide to Fluorescence Probes and Labeling Technologies,* p. 23, Molecular Probes, Inc., Eugene, OR
29. Deivanayagam, C. C., Carson, M., Thotakura, A., Narayana, S. V., and Chodavarapu, R. S. (2000) *Acta Crystallogr. D* **56,** 266–271
30. Qi, Y., Ogunbunmi, E. M., Freund, E. A., Timerman, A. P., and Fleischer, S. (1998) *J. Biol. Chem.* **273,** 34813–34819
31. Samsó, M., and Wagenknecht, T. (2002) *J. Biol. Chem.* **277,** 1349–1353
32. Huang, F., Shan, J., Reiken, S., Wehrens, X. H., and Marks, A. R. (2006) *Proc. Natl. Acad. Sci. U.S.A.* **103,** 3456–3461
33. Cryan, J., Hung, S. H., Wiederrecht, G., Sigal, N. H., and Siekierka, J. J. (1991) *Biochem. Biophys. Res. Commun.* **180,** 846–852
34. Wagenknecht, T., and Samsó, M. (2002) *Front. Biosci.* **7,** d1464–d1474
35. Seidler, T., Loughrey, C. M., Zibrova, D., Kettlewell, S., Teucher, N., Kögler, H., Hasenfuss, G., and Smith, G. L. (2007) *Circ. Res.* **101,** 1020–1029
36. Barg, S., Copello, J. A., and Fleischer, S. (1997) *Am. J. Physiol.* **272,** C1726–C1733
37. Guo, T., Cornea, R. L., Huke, S., Camors, E., Yang, Y., Picht, E., Fruen, B. R., and Bers, D. M. (2010) *Circ. Res.*, in press
38. Amador, F. J., Liu, S., Ishiyama, N., Plevin, M. J., Wilson, A., MacLennan, D. H., and Ikura, M. (2009) *Proc. Natl. Acad. Sci. U.S.A.* **106,** 11040–11044
39. Lobo, P. A., and Van Petegem, F. (2009) *Structure* **17,** 1505–1514